

Stark-modulation-enhanced FM-spectroscopy

P. Werle *, S. Lechner

Fraunhofer Institut IFU, Krenzeckbahnstr. 19, D-82467 Garmisch-Partenkirchen, Germany

Received 27 August 1998; received in revised form 1 September 1998; accepted 12 March 1999

Abstract

Diode lasers are a versatile tool for fundamental atomic and molecular spectroscopy and have increasing applications in gas analysis and diagnostics. In order to obtain quantum limited performance, the problem of the suppression of time-dependent unwanted background structures superimposed to the desired signal from the spectral feature under investigation has to be addressed. Sample modulation enhanced FM-spectroscopy as described in this paper combines laser frequency modulation (FM) with a sample modulation, based on the Stark effect in molecular spectra. The transitions $1_{10}-1_{11}$ at 1746.2 cm^{-1} and $5_{33}-4_{32}$ at 1759.9 cm^{-1} in the ν_2 -band of H_2CO have been used in experiments with static and AC electric fields up to 2 kV cm^{-1} . An intercomparison of the FM technique and the FM-Stark double modulation scheme demonstrates the remarkable potential of this technique for background suppression. © 1999 Elsevier Science B.V. All rights reserved.

Keywords: Tunable diode laser absorption spectroscopy; Sample modulation; Stark effect; Formaldehyde

1. Introduction

The ability to quantify small concentrations of trace gases is an important part of many atmospheric studies being conducted today. Other measurement challenges can be found in medical diagnostics, industrial process control, plasma analysis, kinetical studies and fundamental spectroscopy [1–4]. High demands are, therefore, imposed on analytic instrumentation. Since the absorption spectrum has a fingerprint characteristic for each molecule, spectroscopic methods allow highly specific detection of a broad range of

substances [5]. Diode lasers based on indium phosphite [6,7], antimonide containing compounds [8] and lead-salts [9] cover the spectral range from the visible to the mid-infrared and, therefore, can be used as versatile tunable laser sources for fast and highly sensitive spectroscopic trace gas analysis. This technique is based on the absorption by the fundamental strong vibrational-rotational absorption bands of most gases in the mid infrared spectral region and by overtone and combination bands in the near infrared, where the oscillator strength is typically one to several orders of magnitude weaker than the IR-fundamental band [10,11]. The most important application of diode lasers is their use in conjunction with a longpath cell to provide high sensitivity local mea-

* Corresponding author.

E-mail address: werle@ifu.fhg.de (P. Werle)

surements, when a single narrow laser line scans over an isolated absorption line of the species under investigation. Modulation techniques have made it possible to detect absorptions below 10^{-6} for integration times of about 1 s [12]. This sensitivity, when combined with an optical pathlength through an absorbing sample of several tens of meters, translates into parts-per-billion (ppb) to parts-per-trillion (ppt) detections for many molecular species in the infrared and for many gases with near-IR absorption (overtone or combination) bands, this sensitivity corresponds to detection of subparts-per-million (ppm) concentrations over pathlengths of a few meters.

When the wavelength of the diode laser is tuned over an absorption line, a periodic, often time dependent, fringe structure is superimposed on the desired signal from the absorption of the target gas ('etalon-effect'). For all spectroscopic techniques the problem of fringe reduction remains the main challenge in order to improve sensitivity [13]. An effective fringe-reduction technique requires selective modulation of the sample spectral feature under investigation without affecting fringes and background structure. This modulation has to be faster than the optimum time constant derived from the Allan variance analysis [14]. The standard approach is to switch between ambient and background signals in order to suppress the background fluctuations by subtracting them out. This 'sample modulation' is very slow and especially for sticky, polar substances the exchange time can be very long. It also reduces the duty cycle of the measurement often below 50%. Therefore, a promising approach is the use of an additional fast sample modulation to separate disturbing background effects from the molecular feature of interest [15]. This has been demonstrated in atomic-absorption spectrometry by Niemax and co-workers, who combined wavelength modulation spectroscopy in the near infrared with a plasma modulation for the detection of chlorine atoms at 837.6 nm [16]. Sample modulation schemes, which have been applied in molecular spectroscopy are photochemical modulation [17], magnetic rotation spectroscopy (MRS) for paramagnetic molecules (O_2) [18–22] and photoacoustic spectroscopy (PAS)

using Stark modulation for the detection of NH_3 [23–26]. Line tunable fixed frequency lasers, such as CO, N_2O , and CO_2 , are often used in PAS because they offer High output power, efficiency and reliability. The Zeeman or Stark effect has been used for fine tuning a nearby absorption line into coincidence with a fixed frequency laser. Such a laser Stark spectrometer based on a CO_2 laser has been applied for the measurement of ammonia in flue gas [27]. Optical Stark-modulated absorption spectroscopy of CO using a tunable IR diode-laser and a pulsed Nd: YAG laser has been demonstrated in a flame and in a room temperature absorption cell [28]. Laser stark spectroscopy has been widely used for the exact determination of molecular parameters [29]. Webster et al. applied tunable diode laser stark modulation spectroscopy for the rotational assignment of the HNO_3 7.5- μm band [30]. For the measurement of electric dipole moments the Stark effect was used for example to shift the molecular absorption lines of H_2CO to the fixed nearby laser lines of a fixed frequency CO laser [31,32].

In general the Stark shift and splitting can be used to enhance the specificity of detection of certain gases, because it minimizes the effect of interfering absorbing species which have no electric dipole moment. In order to provide a sample modulation available for a multitude of molecules in addition to laser source high frequency modulation we applied the Stark-effect [33], because important molecules as ammonia, nitric acid, formaldehyde, hydrogen peroxide, hydrogen fluoride and many others show a permanent electric dipole moment, which is a prerequisite for interaction with an external electric field. Laser Stark spectroscopy [34] takes advantage of the fact that a given electric dipole moment of a molecule interacts with an external electric field. This interaction causes a splitting and shift of the energy levels of this molecule. As a result of this influence, the sample, more precisely the lineshapes of the observed absorption transitions, can be directly manipulated by the means of an external electric field. For example, to shift the lines with an static electric field or to modulate it by the application of an alternating field strength.

In this work we investigate the Stark effect in the ν_2 -band of formaldehyde [35,36] in order to provide an sample modulation in addition to laser frequency modulation. The ultimate goal is to improve the system stability and to achieve quantum limited performance of the spectrometer. While laser frequency modulation provides the prerequisite for low noise detection, the additional Stark sample modulation is used to cope with time dependent background structures and fringes. Besides formaldehyde, which is investigated in this work, some other molecules suited for this type of sample modulation enhanced FM-spectroscopy are listed in Table 1.

2. Selective sample modulation based on the Stark effect

In this section we give a brief introduction to the Stark effect in molecular spectra [29] before describing the FM-Stark double modulation principle. In an external electric field, only certain orientations of the total angular momentum J of the molecule are possible such that the component in the field direction is M/\hbar , where $M = J, J - 1, \dots, -J$. If the molecule possesses an electric dipole moment μ , that is, if an interaction with the electric field exists, the states with different M have somewhat different energies $W = W_0 - \bar{\mu} \cdot E$, where W_0 is the energy of the molecule in the absence of the electric field E and $\bar{\mu}$ is the mean value of the electric dipole moment in the field direction. While for symmetric top molecules the mean value of the electric dipole

moment can be calculated for a given set of quantum numbers using $\bar{\mu} = \mu \cdot K \cdot M/J \cdot (J + 1)$, where K is the projection of the angular momentum on the molecular axis, the mean value of the electric dipole moment vanishes in general for asymmetric top molecules. For this kind of molecules a quadratic Stark effect arises, where the splitting of the levels is proportional to the square of the field intensity and which is in general very much smaller than the linear effect. In addition a rather important and interesting special case occurs when two ‘interacting’ levels lie rather close together. This occurs typically for slightly asymmetric top molecules. In this case the energy when a perturbing electric field is applied is given by

$$\Delta W = \frac{\delta}{2} \left[\sqrt{1 + \left(\frac{2E\mu_{12}}{\delta} \right)^2} - 1 \right] \quad (1)$$

where $\delta = W_1^0 - W_2^0$ is the difference in energy of the unperturbed levels and μ_{12} is the dipole matrix element between the two interacting levels. For a slightly asymmetric rotor, the dipole matrix element is fairly accurately given by that of a symmetric top molecule, given above. Because of the $1/J \cdot (J + 1)$ dependence of the dipole matrix element low quantum numbers J and high K 's are preferred. Formaldehyde is a slightly asymmetric prolate rotator. This means that only the second order Stark effect arises, where the most effective Stark effect on spectral lines will be observed for transitions with the projection of the total angular momentum on the molecular axis, K , nearby J (high K or $K \cong J$). This implies that the transitions involve energy levels with only a small K -type doubling and therefore the observed energy levels will have nearby levels. Consequently, the theory simplifies to the description of the plain quantum-mechanical interacting two level system. The Stark shift of the individual M -components of a transition results in

$$\Delta v(E) = (\Delta W_{\text{ex}} - \Delta W_{\text{gr}})/h$$

where ΔW_{ex} and ΔW_{gr} are the Stark splittings of the excited and ground state of the observed transition, which can be calculated with Eq. (1) using the corresponding quantum numbers and dipole moments. Consequently the application of an electric field causes a splitting of a molecular

Table 1
Some molecules suited for the FM-Stark laser sample double modulation scheme

Gas	μ (Debye)	$\bar{\nu}_0$ (cm^{-1})	λ (μm)	$S/10^{-20}$ (cm/molec)
H ₂ CO	2.34	2781.035	3.596	5.9
H ₂ O ₂	2.26	1284.205	7.787	4.5
HNO ₃	2.17	1694.321	5.902	2.9
NH ₃	1.47	930.757	10.744	52
HCl	1.18	2944.914	3.396	50.3
NO ₂	0.29	1600.413	6.248	21.8
N ₂ O	0.17	2236.224	4.472	100.4

transition into $J + 1$ components for a transition with $\Delta M = 0$, or accordingly in $2 \cdot J + 1$ for a $\Delta M = \pm 1$ transition. Combining the two above mentioned effects, splitting of an absorption line in several components, each with different relative line strength and shift of the center frequency of each component, leads to an asymmetry in the convolution of the absorption line, dependent on the applied electric field strength. For a Lorentzian line shape the absorption component reads

$$\delta(E, v) = \sum_{M=0}^J \frac{S_M \cdot \Gamma_{1/2}^2}{\Gamma_{1/2}^2 + [v_0 + \Delta v_M(E) - v]^2} \quad (2)$$

where S_M is the relative intensity of the M th component, $\Delta v_M(E)$ is the frequency shift caused by the electric field E , $\Gamma_{1/2}$ is the HWHM, v_0 is the center frequency of the transition without Stark splitting and v is the observed frequency. The dispersion component can be written similarly. The application of a sinusoidal modulated external electric field like

$$E(t) = \frac{1}{2} E_0 (1 + \sin(\omega_{ST} t))$$

with the Stark modulation frequency ω_{ST} , leads to a time dependence of the Stark shift $\Delta v(t) = \Delta v(E(t))$ and, therefore, a time dependence of the deformation of the absorption line:

$$\delta(t, v) = \sum_{M=0}^J \frac{S_M \cdot \Gamma_{1/2}^2}{\Gamma_{1/2}^2 + \left[v_0 + \Delta v_M \left(\frac{1}{2} E_0 \cdot (1 + \sin \omega_{ST} t) \right) - v \right]^2} \quad (3)$$

In order to combine the Stark sample modulation with laser frequency modulation, we have to look at the signal provided at the rf-mixer output. For a frequency modulated laser emission impinging on a square law detector a current at the mixer IF output (Fig. 1a) we obtain

$$i_{IF} = A(t) \cdot \cos \theta + D(t) \cdot \sin \theta \quad (4)$$

where θ is the phase shift for phase sensitive detection and A and D are the, in general complicated, absorption- and dispersion components of the detected signal, respectively [1]. These compo-

nents depend on the FM modulation index β , the amplitude modulation index m (usually denoted as M , but in this context replaced in order to avoid confusion with the quantum numbers) and the AM/FM phase shift ψ . For low modulation conditions ($\beta \ll 1$, $m \ll \beta$) and $\psi = \pi/2$, Eq. (4) simplifies to $A \cong \beta \cdot (\delta_{+1} - \delta_{-1}) = \beta \cdot \Delta\delta$ and $D \cong \beta \cdot (2\phi_0 - \phi_{-1} - \phi_{+1}) = \beta \cdot \Delta\phi$, where now A is the difference in absorption experienced by the upper and lower sideband multiplied with the FM modulation index β and accordingly D is the difference between the carrier phase shift and the sum of the sideband phase shift multiplied with β . While in the pure FM experiment $\Delta\delta$, and therefore A , and equivalent $\Delta\phi$ and D are stationary, with the additional Stark modulation these two signal components become time dependent. The absorption coefficients at the upper and lower sidebands $\delta_{+1}(t)$ and $\delta_{-1}(t)$ can be calculated with Eq. (3) and therefore we obtain for the current at the mixer IF output port:

$$i_{IF} = \beta \cdot [\delta_{-1}(t) - \delta_{+1}(t)] \cdot \cos \theta + \beta \cdot [\phi_{-1}(t) + \phi_{+1}(t) - 2\phi_0(t)] \cdot \sin \theta. \quad (5)$$

While this detector signal has the same frequency behavior and a constant phase shift as the Stark modulation signal, the detector signal can be phase sensitive detected by the use of a lock-in amplifier that supplies the first Fourier component of the FM-Stark modulation signal, if detection is performed exactly at the reference frequency, that is, at the Stark modulation frequency ω_{ST} . Disturbing components, including signals from fluctuating background, at all other frequencies will be removed by the following low pass filter.

3. Experimental set-up for sample modulation enhanced FM-spectroscopy

The laser-sample modulation approach described in this paper is based on the high frequency modulation technique [1]. A schematic view of the experimental setup is shown in Fig. 1a, b with the Stark modulation extension in the lower right part of Fig. 1a. The FM setup con-

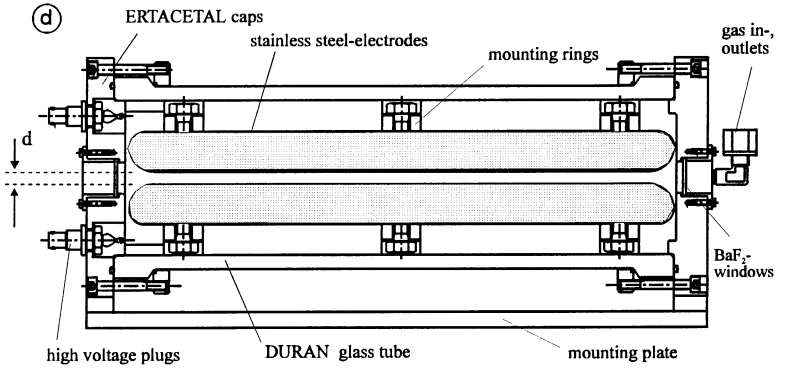
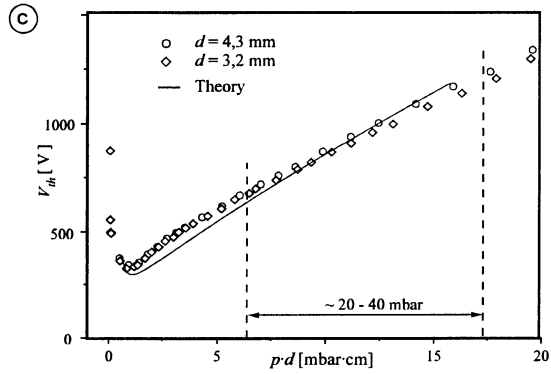
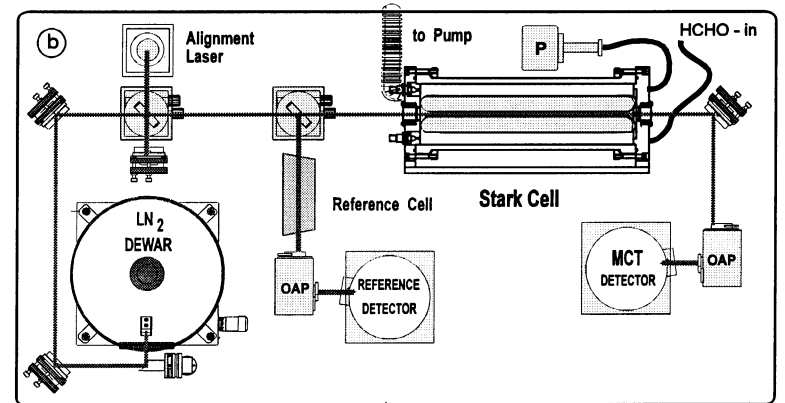
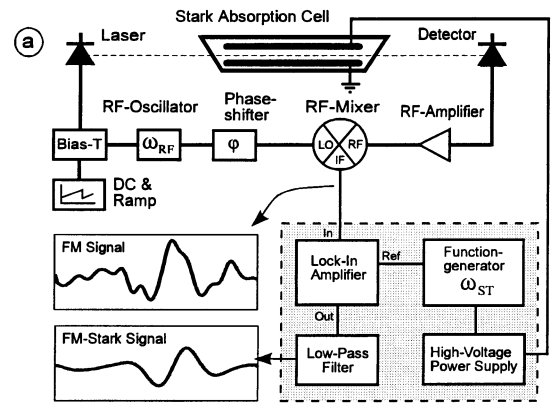


Fig. 1. (a) Experimental setup with the Stark modulation extension; (b) layout of the optical system; (c) experimental data and the Paschen curve; (d) schematic drawing of the 35-cm single pass Stark cell.

tains a lead-salt diode-laser (Laser Photonics) emitting in the ν_2 -band of formaldehyde and mounted in a liquid nitrogen cooled dewar (Laser Photonics, Model 25736). The laser beam is collimated by an off axis parabolic mirror (OAP) before it enters the Stark absorption cell. An integrated laser control system which has been developed at our institute provides the temperature stabilization of the lead-salt diode-laser and supplies a computer controlled current ramp superimposed to a DC-current offset in order to scan the laser wavelength over a single absorption line with a repetition rate of 20 Hz. Frequency modulation and demodulation of the detector signal are performed by a special radio-frequency lock-in amplifier allowing to adjust several FM parameters such as modulation frequency, -phase and -power. An optimum signal has been detected by a modulation frequency of 139 MHz and a cell pressure of 25 mbar. The absorption signal is detected after passing through the Stark absorption cell by a broadband, high frequency HgCdTe photovoltaic detector (SAT). The detector signal is amplified with a 60 dB gain by a low noise, broadband amplifier (SAT, IR500), before it is processed in the demodulation part of the rf-lock-in amplifier. By the use of a beam splitter a part of the laser power is directed through a reference cell on a second HgCdTe detector. This signal experiences no Stark modulation and is used for locking the diode laser frequency to the observed absorption line, to compensate slow drifts in temperature and current of the lead-salt diode-laser. Both signals, the FM signal and the FM-Stark signal are low pass filtered by the same filterbandwidth of 125 Hz (Ithaco, Model 4302). Finally the output signal is sent to a computer for further averaging and storage. Averaging of 64 individual scans led to an effective detection bandwidth of about 2 Hz. The data acquisition time for a concentration value was 3.2 s and the repetition rate was 6 s due to the transfer and storage of all individual spectra and control channels. The additional setup also includes as the main component a special Stark absorption cell, which has been designed to generate a strong electric field perpendicular to the laser beam. The layout of the Stark absorption cell is given in Fig. 1d. A borosilicate glass tube (Schott, DURAN) with an inner diameter

of 10 cm contains the stainless steel electrodes that are responsible for the generation of the electric field. The electrode mounting also works as insulation and therefore is made out of ERTACETAL. These three ERTACETAL rings guarantee a uniform distance between the surfaces of the two electrodes. The gap between the electrodes has been chosen to be 4.35 mm to obtain an optimum between the laser power passing through the gap and the electric field strength. The dimensions of the electrodes are $350 \times 70 \times 26$ mm, whereas the optical path inside the cell is 364 mm. This leads to a ratio of about 0.96 of the overall optical pathlength to the path filled with electric field. The cell is closed at both ends with ERTACETAL caps, in which two BaF₂-windows and the 1/4" gas in- and outlets (Swagelok) are incorporated. The high voltage is introduced into the cell by vacuum tight high-voltage plugs. The connection to the electrodes is maintained by screws placed at the backside of each electrode. The cell can be directed in both ways of electric field polarization by simply rotating the cell by an angle of 90° on its optical axis.

A prerequisite for the application of high electric fields inside the cell is a uniform field distribution between the electrodes. Therefore to achieve a minimum of field distortion a radial edge with a radius of 16 mm has been chosen for the shape of the electrodes. The surface roughness was smoothed by polishing to avoid peaks of the electric field strength that give rise to electrical breakdown. But even for a perfectly uniform field distribution there is a limitation for the applicable voltage, above which electrical breakdown inevitably occurs. This threshold voltage V_{th} , which states an upper limit for the generation of an electric field for a given electrode distance, can be calculated by Paschen's law [37]. In principle an electrical breakdown is based on the multiplication of electron avalanches in the electrode gap. A self-sustained current will be achieved, when the reproduction of electrons, by electron-impact on gas molecules and ion-cathode impact, equals the electron loss by removal from the field. Obviously, at elevated pressures and large gaps an electron can produce numerous ionizing collisions and, therefore, the breakdown voltage is rather low. On the

other hand the possibilities for collisions are very limited at low pressure and small electrode gaps, and for that reason a strong field that involves a large ionization coefficient is required to achieve the necessary amplification. In Fig. 1c the calculated threshold voltage, according to Paschen's law for a uniform field distribution, is plotted as a function of the value of $p \cdot d$, where p is the pressure in the cell and d is the distance between the electrodes. Therefore, Stark spectroscopic experiments have usually been performed by electrode distances less than 1 mm and pressure intervals in the mbar regime. Unfortunately the pressure interval for the optimum FM-Stark signal [20–40 mbar] is very near to the minimum of the threshold voltage. Where the distance between the electrodes d is fixed, as mentioned above, by the optimum of laser power and electric field strength, while the parameter p , that is the pressure in the cell, has to be on the one hand low enough to avoid pressure broadening of the absorption line and on the other hand, since it is proportional to the molecule's concentration, should provide enough optical thickness for measuring low concentrations of trace gases. Nevertheless, the measured breakdown voltage of our Stark electrodes corresponds very well to the theoretical values, evidence that our chosen simple radial edge for the shape of the electrodes implied no drawbacks to the applicable electric field strength. The stainless steel electrodes are connected to a high voltage power supply (Burleigh, RC-45 CFT) which allows the generation of voltages up to 1 kV. This power supply is modulated via its external-modulation input by the use of a function-generator (Rohde & Schwarz, ADS). The modulation is performed with a sine waveform by a modulation frequency of 970 Hz. With regard to the insensitivity of the quadratic Stark effect to the sign of the electric field, the sine wave is applied with an offset of $V_{pp}/2$ to provide only positive field strengths. The peak amplitude of the modulation voltage was chosen to be well below the threshold voltage to inhibit electrical breakdown. The phase sensitive detection of the additional Stark modulation is performed by the use of a supplementary lock-in amplifier (Stanford Research, SR530) referenced to the Starkmodulation frequency (1 f), that is 970

Hz. Therefore the output signal of the rf-lock-in amplifier is directly fed into the input of this second lock-in amplifier to demodulate the additional influence of the applied AC-electric field on the absorption of the molecule. Subsequently the FM-Stark signal is lowpass-filtered and sent to the computer for storage.

4. Experimental results

We applied the combined laser sample double modulation technique based on the Stark effect to formaldehyde (HCHO), which is of interest in atmospheric chemistry and well suited for our investigations due to its strong electric dipole moment of 2.33 Debye in its ground (v_0) Istate. In a first static experiment we looked for absorption lines in the v_2 -band of formaldehyde shown in Fig. 2a, which show an efficient reaction to the application of an electric field, and which can be covered by the emission characteristic of the lead-salt diode-laser. From the mode map shown in Fig. 2b we see that single mode emission has been found near 1746 and 1758 cm^{-1} . Fig. 2c shows the Stark splitting of the transition $1_{11} - 1_{10}$ from the v_2 -band of formaldehyde and Fig. 2d shows a calculated absorption spectrum calculated for some transitions centered around 1753.93 cm^{-1} .

In order to obtain an impression how the Stark effect influences the absorption lines of formaldehyde, we applied a static electric field and observed the reaction of the FM signal. In Fig. 3a this Stark shift is shown for the transition $1_{10} - 1_{11}$ at 1746.16 cm^{-1} for various electric field intensities. The upper part shows the periodic signal produced by a Ge-etalon with a length of 10 cm that was used for frequency calibration. The center frequency shows a shift up to 570 MHz at 2070 V cm^{-1} . This value corresponds very well to the theory describing a $\Delta M = 0$ transition. Likewise according to the Stark theory the signal consists almost completely of the transition $M = 1$ to $M = 1$ while the transition $M = 0$ to $M = 0$, which of course is not shifted by the electric field, has the relative intensity zero, that means it is forbidden by the selection rules. The decrease in signal amplitude is due to the incomplete polarization of

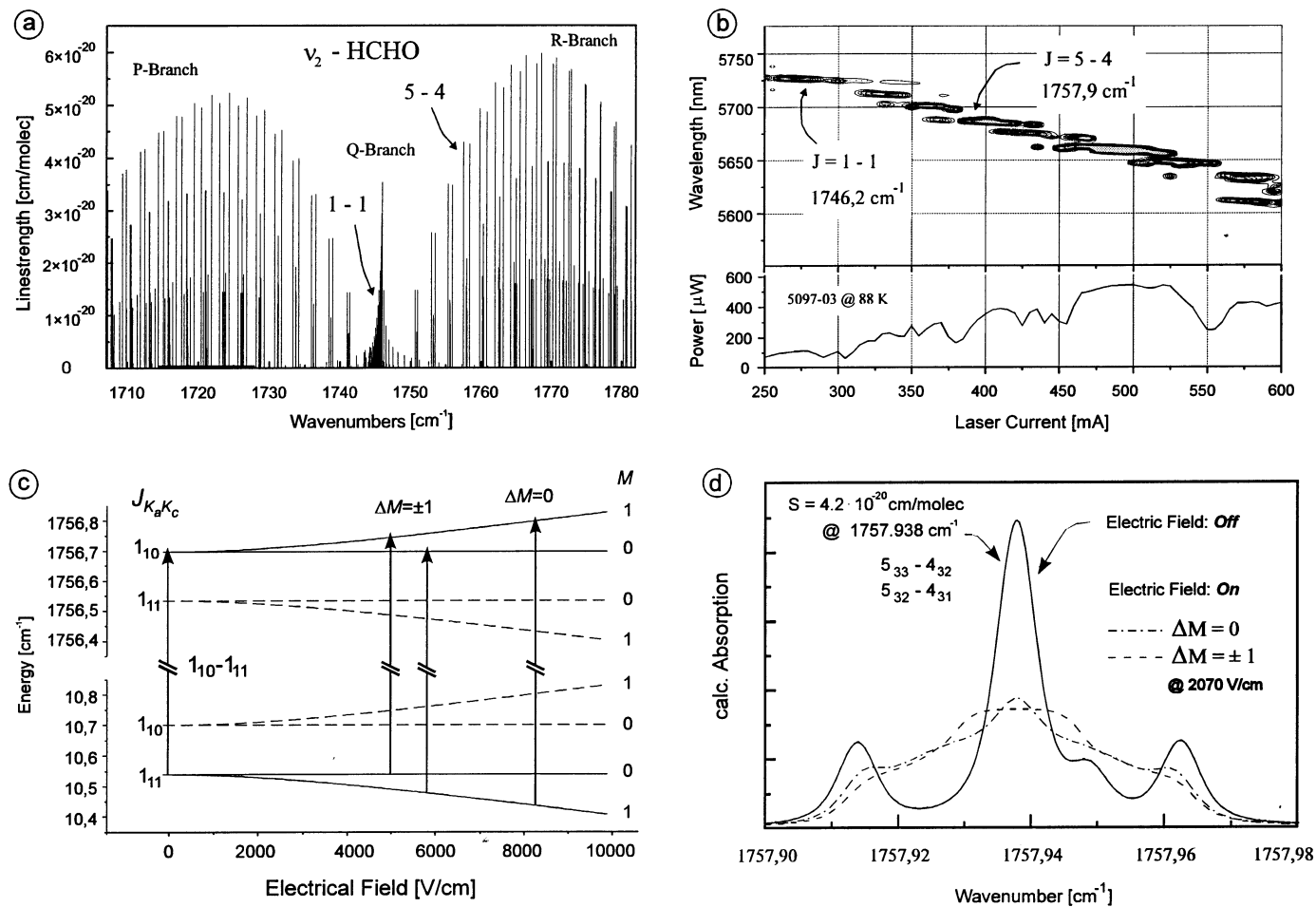


Fig. 2. (a) ν_2 -band of HCHO with the selected lines for Stark shift and Stark modulation experiments; (b) mode map and laser output power versus injection current at 88 K; (c) Energy level diagram for formaldehyde and (d) calculated absorption spectrum for the selected transition at 1757.938 cm^{-1} .

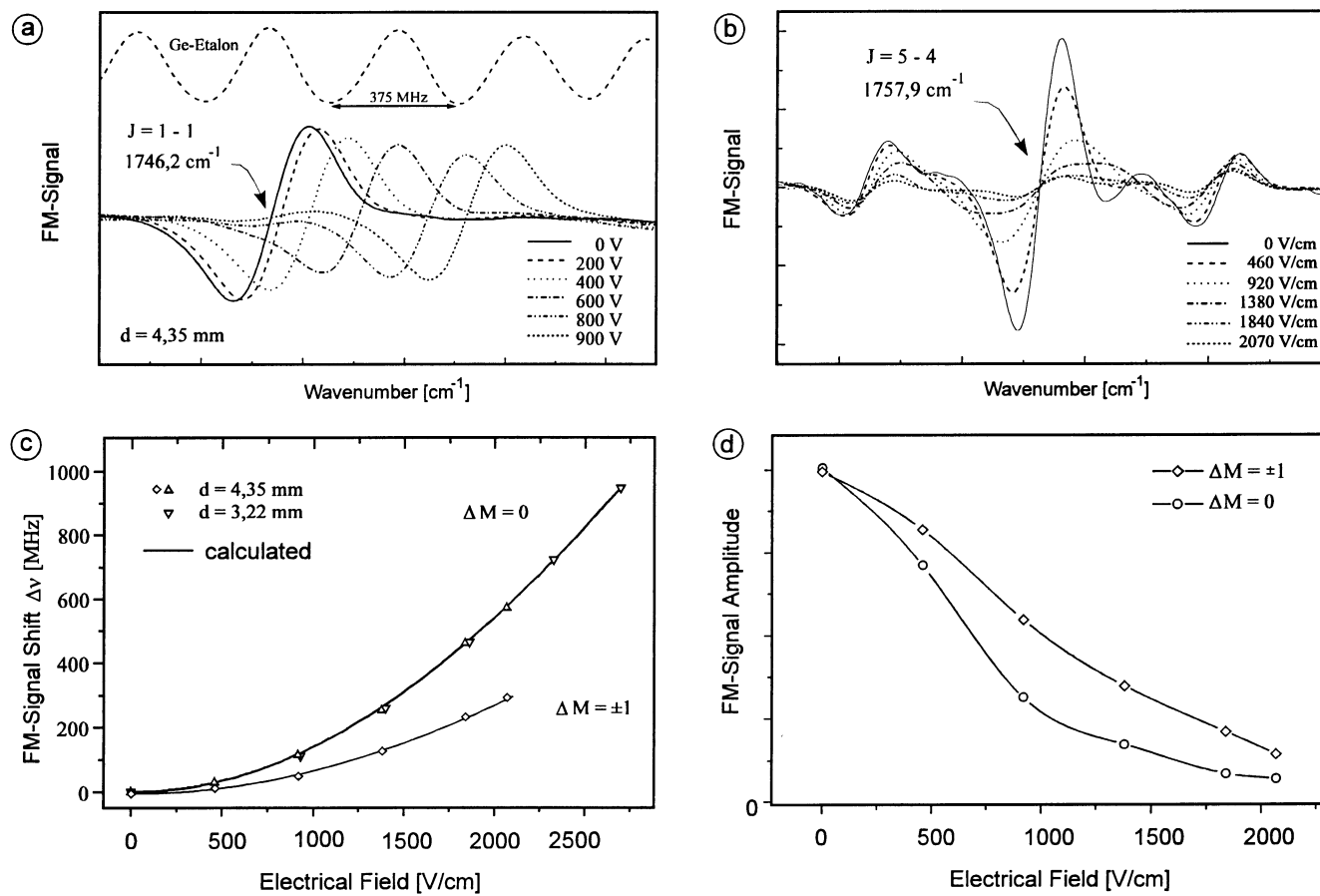


Fig. 3. (a) Stark shift for the $J=1-1$ transition at 1746.2 cm^{-1} and (b) Stark modulation for the $J=5-4$ transition at 1757.9 cm^{-1} for different electrical fields (c) calculated frequency shift and experimental data for $\Delta M=0$ and $\Delta M=\pm 1$; (d) FM signal amplitude under Stark modulation for different electrical fields.

the lead salt diode laser of about 80%, which involves $\Delta M = \pm 1$ transitions being only shifted by halves, and due to the fact that not the complete optical pathlength is filled homogeneous with the electric field as mentioned in the experimental section.

Unfortunately the absorption line at 1746.16 cm^{-1} has only a line strength of $1.5 \cdot 10^{-20} \text{ cm molecule}^{-1}$ and is therefore too weak for detecting trace gas concentrations. For that reason we searched for a second, more suitable absorption line. In accordance to the theory of the Stark splitting, we had to look for transitions with high quantum numbers K_a and low J . We found that an absorption at 1757.94 cm^{-1} , consisting of an absorption line doublet in the *it*-branch of the band, with the transitions $5_{32}-4_{31}$ and $5_{33}-4_{32}$ and a line strength of $4.2 \cdot 10^{-20} \text{ cm molecule}^{-1}$, shows a strong Stark splitting. In Fig. 3b the FM-signal of this absorption line doublet is shown without an electric field and with an increasing electric field of up to 9070 V cm^{-1} . Caused by the strong splitting of the involved energy levels of these transitions, the FM line shape experiences a great deformation, which leads to an almost complete disappearance of the FM-signal. This strong reaction on the application of an external electric field has been enabled by the very small difference in energy of the nearby ground states $\delta_{\text{gr}} = W^0(4_{32}) - W^0(4_{31}) = 1 \cdot 10^{-4} \text{ cm}^{-1}$ and of the excited states $\delta_{\text{ex}} = W^0(5_{32}) - W^0(5_{33}) = 6 \cdot 10^{-4} \text{ cm}^{-1}$, which are involved in the denominator of equation (1). Instead of a simple shift of the center frequency, like the previous $1_{10}-1_{11}$ transition, a large deformation of this line can be observed which arises because of the complicated Stark pattern. This Stark pattern is composed, in the simpler case with $\Delta M = 0$, of a splitting of each of these transitions in five components, each with a different Stark shift and a different relative intensity, according to the quantum number M . For $\Delta M = \pm 1$ transitions, which can be selected by simply turning around the Stark electrodes 90° on the optical axis, nearly the same experimental result is obtained, only a slightly smaller decrease in the FM-signal amplitude was measured.

Because of the efficiency of the Stark splitting of this absorption line doublet, the same transition has been chosen for dynamic FM-Stark double modulation experiments. For this kind of measurements a sinusoidal AC-high voltage has been applied to the electrodes of the Stark absorption cell, whereas the same modulation signal was fed at the same time in the reference input of the lock-in amplifier, which was used for phase sensitive detection of the Stark modulated signal provided at the rf-mixer output. Accurate optimization of the FM-Stark double modulation signal has been performed. The crucial parameter is the pressure in the absorption cell. We have to balance between high pressure with large optical depth and little elevated threshold voltage, but pressure broadening of the linewidth and on the other hand low pressure with narrow lines, and, therefore, a larger Stark modulation coefficient and higher selectivity, but connected with a decrease in the applicable breakdown voltage. The Stark modulation coefficient is defined as the ratio of the Stark splitting to the line halfwidth at half maximum (HWHM). The optimum FM modulation frequency for FM-Stark modulation differs barely from the optimum (plain) FM frequency for the given experimental setup. The optimum signal for the observed absorption line doublet at 1757.94 cm^{-1} could be achieved by a pressure in the cell of 25 mbar, a maximum Stark modulation amplitude of 2070 V cm^{-1} , limited by electrical breakdown, and a Stark modulation frequency of 970 Hz, whereas the FM frequency was 139 MHz. Experiments have also been performed with the direction of the electric field parallel and perpendicular to the polarization of the diode laser beam, which enables selection between transitions with $\Delta M = 0$ and $\Delta M = \pm 1$, respectively. For the first orientation, that is the polarization of the laser parallel to the electric field lines, a slightly enhanced signal amplitude of the FM-Stark double modulation signal of about 5% could be observed.

In order to compare the conventional FM technique and the FM-Stark double modulation technique, we recorded time series data obtained from the measurement of a constant formaldehyde concentration provided by a calibration source. The

measurements for both techniques have been done in the same manner. First the absorption cell was flushed with zeroair to record possible background structures, which are subtracted from the current ambient air spectra. Then a constant flow of 1 l min^{-1} (STP) air through the cell has been established. During all measurements the cell pressure has been actively stabilized to 25 mbar. We adjusted the mixing ratio of formaldehyde to attain an optical depth of $4.1 \cdot 10^{-4}$ for the 35 cm pathlength, which is comparable to the usual optical depth working with multipass cells for trace gas analyses. With this constant gas flow of 4.6 ppm HCHO first a calibration spectrum has been recorded, which we assigned the relative concentration 1.0. In the following further sample spectra have been recorded with the same volume mixing ratio with a repetition rate of 6 s and an effective bandwidth of 2 Hz. A successive fitting algorithm, using the multiple linear regression analysis, calculated the time series concentration data [1].

The intercomparison of the pure FM technique and the double modulation scheme is illustrated in Fig. 4, where typical spectra for both techniques are shown. Obviously the FM signal (Fig. 4a) superimposed has a periodic fringe structure. The amplitude of the fringe corresponds to an optical density of $3 \cdot 10^{-5}$ s. From the free spectral range of 81 MHz the resonator length was calculated as 1.85 m, which is exactly the distance between the laser and the detector. In contrast, the FM-Stark signal (Fig. 4d) is very smooth, indicating no symptom of interfering étalon fringes. In order to get an impression of the signal stability we have recorded FM spectra and combined FM-Stark double modulation spectra, which are both shown in the isoplot in Fig. 4a, d. While the drift effects caused by moving fringe structures can be clearly identified in the FM-signal, a significantly higher stability has been obtained after the application of the double modulation scheme. The system stability according to the calculated time series concentration values has been characterized by the Allan variance [14]. For that purpose the Allan variance has been plotted as a function of the averaging time. In doing so we get at the minimum of the Allan

variance the optimum averaging time, which is a characteristic for a given instrument, in particular in our case for a given measurement method. Fig. 4c shows the FM measurement, which indicates a significant decline of the recorded time series data of the relative HCHO concentration, although a constant value would have been expected. This strong drift has obviously been caused by the presence of fluctuating background structures such as a moving fringe. The negative influence of this signal drift finds its equivalent in the corresponding Allan plot shown in Fig. 4c. Up to 24 s signal averaging leads to a linear decrease of the Allan variance, with the minimum value of $1.7 \cdot 10^{-5}$. Beyond this optimum integration time the Allan variance, and with it the instrument's detection limit, will deteriorate as a consequence of disturbing background drifts. It should be emphasized, that the minimum of the Allan variance indicates the optimum integration interval, within both background spectrum and ambient air spectrum recording has to be completed. For recording of the ambient air spectrum only less than half of the overall integration time is available due to the required gas exchange times.

In contrast to this FM measurement, the relative concentration recorded with the FM-Stark double modulation technique presented here (Fig. 4e) exhibits almost no deviation from the expected constant value. Only slight changes in the noise of the relative concentration values can be noticed. The calculated Allan variance emphasizes this behavior (Fig. 4f). Starting with an increased value, the Allan variance declines linearly with the integration time reflecting a white-noise dominated region. The FM-Stark double modulation technique yields an optimum integration time of 120 s which is five times the optimum integration time of the mere FM technique. Strongly correlated with this enhanced integration time is a notable gain in the Allan variance by a factor of more than three to a value of $5 \cdot 10^{-6}$. For integration times beyond 120 s the Allan plot shows a horizontal level, which indicates the presence of 1/f-type noise. Further averaging will not help to improve the detection limit. Probably this 1/f-type noise will be caused by the turbulent gas flow through the absorption cell which is strongly re-

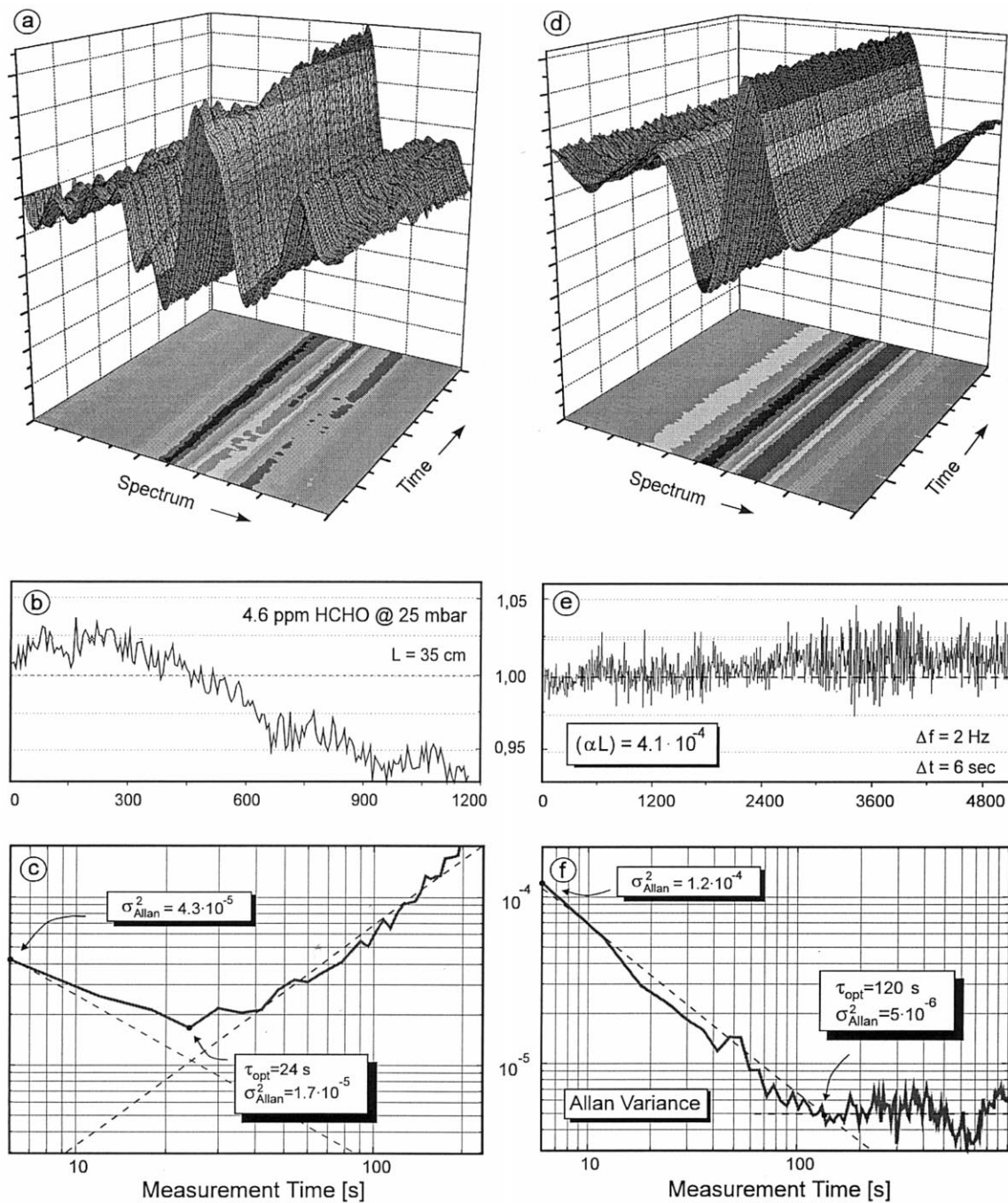


Fig. 4. Comparison of the FM technique (left side) and the FM-Stark laser-sample double modulation technique (right side): (a) FM spectra with a superimposed time dependent fringe structure; (b) time series data from a 4.6 ppm formaldehyde calibration gas; (c) Allan plot; (d) FM-Stark spectra; (e) related time series data and (f) corresponding Allan plot. For both measurement series the optical density (αL) was adjusted to $4.1 \cdot 10^{-4}$ at 25 mbar and the detection bandwidth was 2 Hz.

lated to refractive index fluctuations [38]. Contrary to the FM-technique, where half of the time is lost by recording background spectra, there is no need for background measurement by the FM-Stark technique.

Consequently the whole integration time is available for measurement, thereby doubling the duty cycle of the system. The price we have to pay for this is that the initial Allan variances at 6 s are higher for the double modulation scheme, equivalent to the slightly higher noise in the time series data. In the FM-Stark double modulation case we phase sensitive detect the difference in the FM signals with the electrical field on and off as shown in Fig. 3d, and therefore we always lose some amplitude as the FM signal does not completely disappear. The lock-in amplifier measures the effective signal voltage, which in total reduces the signal-to-noise ratio in comparison to the pure FM technique and, therefore, increases the noise in the time series data. However, due to the increased stability this initial loss can easily be compensated and for longer integration times higher sensitivity can be obtained.

The Allan variance analysis is very convenient for the predictions of sensitivities as a function of integration time [14]. As it has been stated earlier, all measurements were performed at an optical density $(\alpha L) = 4.1 \cdot 10^{-4}$, equivalent to a concentration of 4.6 ppm formaldehyde at 35-cm pathlength. The detection limits can easily be calculated by multiplying the initial optical density (concentration) by the square root of the Allan variance for a given measurement time. For the pure FM technique we obtain from Fig. 4c for 6 s an optical density of $(\alpha L)_{\min} = 2.7 \cdot 10^{-6}$ ($\Delta f = 2$ Hz) equivalent to 30 ppb, and for the optimum integration time of 24 s we obtain $(\alpha L)_{\min} = 1.7 \cdot 10^{-6}$ or 18 ppb. For the FM-Stark double modulation technique we obtain from Fig. 4f for 6 s an optical density of $(\alpha L)_{\min} = 4.5 \cdot 10^{-6}$ ($\Delta f = 2$ Hz) equivalent to 50 ppb and for the optimum integration time of 120 s we obtain $(\alpha L)_{\min} = 9 \cdot 10^{-7}$ or 10 ppb. All these numbers are calculated from recorded data. Any extrapolation beyond the optimum integration time determined for the given experimental conditions leads to meaningless numbers as the rela-

tionship between the sample and background spectra is lost.

5. Summary and conclusions

The problem of baseline drifts is the key issue for the design of ultra-sensitive spectrometers as well as for operational instrumentation for field measurements [39]. Approaches towards achieving the quantum limit use, for example, clever designs of optoelectronic receivers [40], but they do not fully solve the problem of baseline drift. An other example is the so-called cavity-ringdown spectroscopy [41] measuring for a given cavity the field decay time, which is a function of the intracavity absorption once the input laser field is switched off, hence avoiding the laser amplitude noise and, therefore, it appears that the shot noise limit can be approached. Unfortunately, the on-resonance versus off-resonance decay time measurements are separated in time, and it is their difference that contains the desired information. This time separation generates the same problems with system stability as we observe them in tunable diode laser absorption spectroscopy. However, FM spectroscopy is one of the most powerful spectroscopic techniques for ultrasensitive and high-speed detection of weak absorption signals [42]. In principle, FM spectroscopy offers a detection sensitivity limited only by the fundamental quantum noise. In practice, some effects as residual amplitude modulation, laser excess noise and fringes in the optical system exist and limit the ultimate FM sensitivity. A number of techniques have been developed to cope with these problems and double modulation schemes seem to be a well suited approach.

The application of an additional sample modulation using the Stark effect is an efficient method for the suppression of background fluctuations. We demonstrated a substantial improvement of the system stability and useful integration times, which is a prerequisite for improving the detection limits and/or measurement precision. Moreover, because of the lack of interfering background structures, there is no need for background recording and – subtraction and thereby this

technique will provide enhanced duty cycles. The FM-Stark double modulation technique is applicable to molecules with a permanent dipole moment and many molecules which play an important role in the chemistry of the atmosphere exhibit such an electric dipole moment as shown in Table 1. With our 35-cm single path cell we achieved a detection limit of 10 ppbv formaldehyde for an integration time of about 120 s. It has to be mentioned that a single measurement was made within about 3.2 s but the measurements could be repeated only every 6 s due to slow data processing and recording of the individual spectra. This led to a duty cycle of only about 50%, which can easily be increased up to 100%. This in turn will lead to an improvement by approximately a factor of 2 giving a detection limit of 5 ppbv (See Ref. [14] for a detailed treatment of dead-time and duty-cycle). For demonstration purposes we developed a 35-cm single pass cell. For real field applications of course a long path cell has to be applied. If we assume a final path-length of only 35 m we should obtain a further improvement by a factor of 100 and the predicted detection limit would be 50 pptv. This estimation is based upon the data presented. No real attempt was made to stabilize the system and to reduce fringes by proper system alignment as we wanted to demonstrate how effectively the Stark sample modulation can suppress background drifts. This can be seen from the Allan plot of the FM measurements *w/o* Stark modulation, which reports only about 24 s as the optimum integration time, while 60–100 s can be obtained without sample modulation [14,39]. The integration time in the double modulation case was limited to about 120 s due to the presence of 1/f-type noise in the system, which can be attributed either to the presence of spurious side modes during laser operation and/or to the presence of turbulence effects in the cell. It is important to mention that even for longer integration times no significant drift influence (i.e. an increase in the Allan variance at longer integration times) can be observed. Careful laser selection and an optimized cell design should allow longer integration times and, therefore, 50 pptv is a conservative estimate and even a further improvement by a factor of 10 should be

feasible, in principle. In practice, we have reduced the problem to the design of a multipass Stark cell giving the required long absorption path by ‘folding’ the laser beam between two narrow plain steel electrodes.

Acknowledgements

The authors want to thank Robert Mücke and Robert Kormann for stimulating discussions and Bernd Jänker for the help with the design of the Stark-cell. We also want to acknowledge the support of Prof. R. Niessner from the Technical University Munich. This work has been funded by the Bayerische Staatsministerium für Wirtschaft, Verkehr und Technologie.

References

- [1] P. Werle, *Spectrochim. Acta Part A* 54 (1998) 197.
- [2] K. Niemax (Ed.) *Diode Laser Spectroscopy*, *Spectrochim. Acta Rev.* 15 (1993) 289.
- [3] P. Werle, Survey Paper, 5th Int. Symp. Gas Analysis by Tunable Diode Lasers, Verein Deutscher Ingenieure, VDI Berichte 1366, VDI Verlag GmbH, Dusseldorf, 1998, 1.
- [4] A. Fried (Ed.), *Application of tunable diode lasers and other infrared sources for atmospheric studies and industrial monitoring*, *Proc. SPIE* 2834 (1996).
- [5] C. Webster, R.T. Menzies, E.D. Hinkley, in: R.M. Measure (Ed.), *Laser Remote Chemical Analyses*, Wiley, New York, 1988.
- [6] R.U. Martinelli, *Laser Focus World* 3 (1996) 77.
- [7] P. Werle, R. Mücke, F. D’Amato, T. Lancia, *Appl. Phys. B* 67 (1998) 307.
- [8] P. Werle, A. Popov, *Appl. Opt.* 38 (1999) 1494.
- [9] M. Tacke, *Infrared Phys. Technol.* 36 (1995) 447.
- [10] G. Herzberg, *Molecular Spectra and Molecular Structure*, van Nostrand Reinhold, New York, 1950.
- [11] W. Demtröder, *Laser Spectroscopy*, Springer Verlag, Berlin, 1982.
- [12] P. Werle, F. Slemr, M. Gehrtz, C. Bräuchle, *Appl. Phys. B* 49 (1989) 99.
- [13] P. Werle, *Inf. Phys. Technol.* 37 (1996) 59.
- [14] P. Werle, R. Mücke, F. Slemr, *Appl. Phys. B* 57 (1993) 131.
- [15] P. Werle, *Spectrochim. Acta Part A* 52 (1996) 805.
- [16] V. Liger, A. Zybin, Y. Kuritsyn, K. Niemax, *Spectrochim. Acta Part B* 52 (1997) 1125.
- [17] E.A. Whittaker, H. Wendt, H. Hunziker, G.C. Bjorklund, *Appl. Phys. B* 35 (1984) 105.

- [18] M.C. McCarthy, J.C. Bloch, J.R. Field, *J. Chem. Phys.* 100 (1994) 6331.
- [19] J.M. Smith, J.C. Bloch, R.W. Field, J.I. Steinfeld, *J. Opt. Soc. Am. B* 12 (1995) 964.
- [20] T.A. Blake, C. Chackerian, J.R. Podolske, *Appl. Opt.* 35 (1996) 973.
- [21] R.J. Brecha, L.M. Pedrotti, D. Krause, *J. Opt. Soc. Am. B* 14 (1997) 1921.
- [22] G.A. Laguna, *Appl. Opt.* 23 (1984) 2155.
- [23] H. Sauren, D. Bicanic, W. Hillen, H. Jalink, K.V. Asselt, J. Quist, J. Reuss, *Appl. Opt.* 29 (1990) 2679.
- [24] H. Sauren, E. Gerkema, D. Bicanic, H. Jalink, *Atm. Environ. A* 27 (1993) 109.
- [25] M.J. Kavaya, J.S. Margolis, M.S. Shumate, *Appl. Opt.* 18 (1979) 2602.
- [26] A. Thöny, M.W. Sigrist, *Rev. Sci. Instrum.* 66 (1995) 227.
- [27] A.J.L. Verhage, R.A. Rooth, L.W. Wouters, *Appl. Opt.* 32 (1993) 5856.
- [28] K. Knapp, R.K. Hanson, *Appl. Opt.* 22 (1983) 1980.
- [29] K. Tanaka, Y. Nakahara, M. Yamaguchi, T. Tanaka, *J. Opt. Soc. Am. B* 4 (1987) 1182.
- [30] C.R. Webster, R.D. May, M.R. Gunson, *Chem. Phys. Lett.* 121 (1985) 429.
- [31] J.W.C. Johns, A.R.W. McKellar, *J. Molec. Spect.* 48 (1973) 354.
- [32] C. Bréchnac, J.W.C. Johns, A.R.W. McKellar, M. Wong, *J. Molec. Spect.* 96 (1982) 353.
- [33] C. Townes, A. Schawlow, *Microwave Spectroscopy*, Dover, New York, 1975.
- [34] Y. Ueda, K. Shimoda, in: H. Walther (Ed.), *Laser Spectroscopy of Atoms and Molecules*, Springer-Verlag, Berlin, 1976.
- [35] L.R. Brown, C.B. Farmer, C.P. Rinsland, R.A. Toth, *Appl. Opt.* 26 (1987) 5154.
- [36] D.M. Sweeger, R.L. Sams, *J. Molec. Spect.* 87 (1981) 18.
- [37] Y.P. Raizer, *Gas Discharge Physics*, Springer-Verlag, Berlin, 1991.
- [38] P. Werle, B. Janker, *Opt. Eng.* 35 (1996) 2051.
- [39] A. Fried, B. Henry, B. Wert, S. Sewell, J.R. Drummond, *Appl. Phys. B* 67 (1998) 317.
- [40] P.C.D. Hobbs, *Appl. Opt.* 36 (1997) 903.
- [41] A. O'Keefe, D.A.G. Deacon, *Rev. Sci. Instrum.* 59 (1988) 2544.
- [42] J. Ye, L.-S. Ma, J.L. Hall, *J. Opt. Soc. Am. B* 15 (1998) 6.